Direct Measurement of Facet Temperature up to Melting Point and COD in High-Power 980-nm Semiconductor Diode Lasers

Stephen John Sweeney, *Member, IEEE*, Leslie Jamieson Lyons, Alfred R. Adams, *Fellow, IEEE*, and Daren Alfred Lock

***Abstract*—The authors describe a straightforward experimental technique for measuring the facet temperature of a semiconductor laser under high-power operation by analyzing the laser emission itself. By applying this technique to 1-mm-long 980-nm lasers with 6- and 9-μm-wide tapers, they measure a large increase in facet temperature under both continuous wave (CW) and pulsed operation. Under CW operation, the facet temperature increases from $\sim$ 25 °C at low currents to over 140 °C at 500 mA. From pulsed measurements they observe a sharper rise in facet temperature as a function of current ($\sim$ 400 °C at 500 mA) when compared with the CW measurements. This difference is caused by self-heating which limits the output power and hence facet temperature under CW operation. Under pulsed operation the maximum measured facet temperature was in excess of 1000 °C for a current of 1000 mA. Above this current, both lasers underwent catastrophic optical damage (COD). These results show a striking increase in facet temperature under high-power operation consistent with the facet melting at COD. This is made possible by measuring the laser under pulsed operation.**

***Index Terms*—Laser thermal factors, optical fiber communication, power lasers, semiconductor device measurement, semiconductor lasers, temperature measurement.**

I. Introduction

THERE is an increasing demand for inexpensive high-power semiconductor lasers with applications ranging from domestic use in recordable digital versatile discs (DVD-R) and rewritable compact discs (CD-RW), both of which are now becoming commonplace, for printing and marking technologies, for telecommunications systems, and increasingly in medical applications such as photodynamic therapy, photo-coagulation or ablation, thermal therapy, and for invasive and noninvasive surgery. In each of these applications, high-power visible or near infrared lasers form the essential component due largely to their compact and robust nature. Telecommunications has pushed forward the rapid evolution of high power semiconductor lasers. In particular, the development of erbium-doped fiber amplifiers (EDFAs) gave rise to the need for semiconductor lasers emitting several hundred milliwatts of power at 980 or 1480 nm [1]. More recently, there has been widespread interest in developing distributed Raman amplifiers which offer the advantage of using the existing optical fiber itself as the amplifying medium. In order to produce gain in the important 1530–1560-nm telecommunications C-band, Raman amplifiers require semiconductor lasers emitting in the range $\sim$1430–1460 nm with fiber coupled powers $\sim$0.5 W [1]. Thus, for many applications, output powers of several hundred milliwatts are required frequently giving rise to power densities at the laser facets $\sim$1-10 MWcm^{-2}. Power densities of this magnitude can easily damage many materials; indeed, it is precisely this that makes them suitable for many of their applications. However, power densities of this order at the laser facet can give rise to local facet damage. This damage may either be in the form of locally induced defects which can propagate, thereby reducing the lifetime of the laser, or alternatively it may cause a catastrophic failure of the laser itself. The latter of these problems is commonly known as catastrophic optical damage (COD) and it is the problem of COD in 980-nm pump lasers that we address in this paper. In order to eliminate, or reduce the probability of COD occurring in high power lasers, it is useful to be able to ascertain what is happening at the laser facet at high powers. As we shall discuss in Section II, COD occurs due to extreme heating of the laser facet resulting in the physical melting of a region of the facet itself. Many different laser materials/structures have been considered to minimize the likelihood of COD ranging from strain overcompensation, facet passivation, and stripe/ridge tapering to intermixing at the laser facet [2]–[13]. In order to be able to assess the relative merits of different designs, it is useful to be able to quantify their effectiveness in terms of how well they reduce the rate at which the facet heats up. In this paper, we describe a method of directly measuring the local facet temperature by analyzing the spontaneous emission emerging from the facet. From these measurements we have been able to observe the rate of facet heating with increasing laser bias current/output power up to the point at which the laser undergoes COD. Using this technique, we compared two 980-nm lasers which incorporate linear tapers along the ridge to reduce the power density at the laser facet [14]. From these measurements we find that, for our lasers, the taper had little effect on the current at which the devices underwent COD. We attribute this to the relatively short taper length. Interestingly, with this technique, for these lasers we measured facet temperatures up to the melting point (MP) of GaAs ($\sim$ 1240 °C [15]) under pulsed operation and observed that the temperature increased steadily and superlinearly with increasing current/power up to COD. Our results show that this

Manuscript received February 14, 2003; revised July 23, 2003.
S. J. Sweeney, A. R. Adams, and D. A. Lock are with the Advanced Technology Institute, School of Electronics and Physical Sciences, University of Surrey, Surrey GU2 7XH, U.K. (e-mail: s.sweeney@surrey.ac.uk).
L. J. Lyons is with Bookham Technology, Towcester, NN12 8EQ, U.K.
Digital Object Identifier 10.1109/JSTQE.2003.820912

1077-260X/03$17.00 © 2003 IEEE

Authorized licensed use limited to: University of Surrey. Downloaded on May 26, 2009 at 10:09 from IEEE Xplore. Restrictions apply.

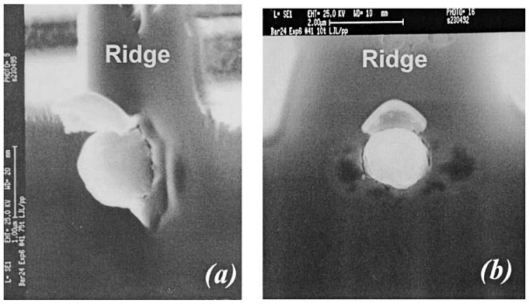

Fig. 1. SEM images of a laser facet having undergone COD. (a) Material near the facet has molten and pushed through the facet before finally resolidifying. The facet coating has been lifted up by the force of the ejected material. (b) Most damage occurs at the center, where the optical field intensity is at a maximum. Also visible is an elliptical pattern where the material has been disturbed corresponding well with the overall shape of the laser near-field pattern.

technique is a very useful tool for the analysis of semiconductor lasers for high power operation.

In Section II, we discuss COD in semiconductor lasers and its wavelength dependence. In Section III, we discuss techniques for measuring the laser facet temperature and discuss the underlying theory behind our chosen technique. In Section IV, we describe the experimental methodology. In Section V, we describe the results of this technique applied to 980-nm lasers under pulsed and continuous wave (CW) operation. Finally, in Section VI we conclude.

II. Catastrophic Optical Damage

One of the greatest challenges in producing long-lived high-power laser diodes emitting at 980 nm is to solve the problem of COD. COD occurs at the facet due to severe heating. Catastrophic failure of the facet arises when the temperature reaches the MP of the semiconductor layers forming the device. Evidence for this can be seen from scanning electron microscope (SEM) images of post-COD laser facets. Fig. 1 shows two typical images of 980-nm lasers that have undergone COD. From Fig. 1(a), the outline of the laser ridge (upper half of the figure) is clearly visible below which a protrusion can be seen. The most plausible cause of this is that, at COD, material close to the facet melts and pushes through. The exact chemical composition of this material is presently unknown and is the subject of ongoing investigations. The mechanics of this are discussed in [16]. It can also be seen that the facet coating has fractured and lifted up due to the force from the molten material. The elliptical pattern evident in the image is consistent with the shape of the near field pattern of the optical mode with the major damage occurring close to the center corresponding to the maximum intensity position of the optical field.

GaAs has an MP of 1240 °C (at atmospheric pressure) and the MPs of related alloys are of similar values [15]. The underlying origin of the facet heating arises due to the strong absorption of the laser radiation close to the laser facet followed by nonradiative recombination and energy transferred to the lattice via the emission of phonons, consequently giving rise to a localized temperature increase. This temperature increase itself leads to bandgap shrinkage, giving rise to further absorption in a self-depreciating manner. Possible causes of the absorption at the laser facet can be due to both intrinsic material properties of the laser and extrinsic properties relating to the environment in which the laser is placed.

Intrinsic properties relate to the structure of the laser itself. Typical 980-nm laser structures consist of highly (>1%) compressively strained QWs within unstrained GaAs barriers surrounded by AlGaAs cladding on a GaAs substrate. This is a convenient means of obtaining 980-nm emission using a GaAs substrate but produces a large net positive strain in the structure. Growing an epilayer, e.g., a quantum well (QW), in a state of biaxial compression requires that the "bulk" lattice constant of the epilayer is higher than that of the substrate, in this case GaAs. During growth, the epilayer is forced to have the lattice constant of the substrate giving rise to a tetragonal distortion in the active region. One of the principal effects on the energy band structure of the QW is an increase in the bandgap. However, close to the facet, this compressive strain will relax, causing the facet to "bulge" slightly outwards. The loss of strain close to the facet therefore causes the bandgap to shrink producing a region of strong absorption. This problem was previously identified in visible Al(GaInP)-based lasers which have even lower COD tolerance than 980-nm devices (Valster *et al.* [4]). Thus, in highly compressively strained QWs, facet absorption is an intrinsic device property. Strain overcompensation techniques can be successfully employed to alleviate this problem as have been discussed in further detail elsewhere [4], [6]. Extrinsic properties of the laser can also strongly influence absorption at the laser facet. These can broadly be divided into two mechanisms. The first of these arises due to the fact that at the laser facet surface states arise due to the dangling bonds of surface layer atoms. Without passivation, these states are susceptible to oxidation which produces further absorption centers [2]. Band structure changes at the interface (unrelated to strain) may also complicate the absorption spectrum. Secondly, impurities present on the laser facet which themselves do not interact chemically with the semiconductor may still absorb laser radiation and give rise to localized heating. Cleaning of the laser facet prior to coating is, therefore, a key aspect of laser processing [3]. QW intermixing at the laser facet can also reduce absorption due to the local increase in bandgap at the laser facet [11].

One might expect that facet absorption and COD will occur in any semiconductor laser operating at high power. However, this appears not to be the case, as evident from the literature. COD is known to be a significant problem in Al(GaInP)/GaAs visible lasers and InGaAs–GaAs devices. However, InP-based devices such as those emitting at the telecommunications wavelengths (~1.3 and ~ 1.5 μm) seem immune to COD. Such devices are based upon InP, rather than GaAs as used for the shorter wavelength devices. It may be that the increased thermal conductivity of InP (0.68 $WKcm^{-1}$ [17]) compared with GaAs (0.44 $WK^{-1}cm^{-1}$ [17]) makes heat dissipation more effective. In addition, the surface recombination velocity of InP is two orders of magnitude lower than that of GaAs, and hence surface defect-related current paths are likely to be considerably more important in GaAs [18]. Long wavelength InP-based devices also tend to suffer from overall device heating due to intrinsic inefficiencies as a result of dominant nonradiative loss

Authorized licensed use limited to: University of Surrey. Downloaded on May 26, 2009 at 10:09 from IEEE Xplore. Restrictions apply.

processes [19], [20]. Thus, under normal operating temperatures, it is likely that such devices rollover before reaching the COD threshold for the material. Other possible explanations may be due to the much lower photon energies (∼0.8–1.0 eV for long wavelength devices compared with ∼1.2–2.0 eV for 980 nm and visible devices, respectively) so that less energy needs to be dissipated into the lattice following absorption. Differences in phonon energies between the two materials systems will also influence the rate at which energy is dissipated. A detailed discussion of such effects can be found in the review paper of Eliseev [21].

III. Determining Facet Temperature

In order to ascertain the degree to which absorption and consequently facet heating affect different laser structures, it is useful to be able to measure the local temperature at the laser facet (T_f). Such a measurement can then be used to compare laser variants such as QW/barrier compositions, cavity lengths, taper widths, facet coatings, intermixed facets and so on, which themselves will, to varying extents, influence heat dissipation. While it is reasonably straightforward to estimate the *junction* temperature as a function of current/power (e.g., from the thermally induced shifts in the laser emission wavelength) it is a considerably more difficult task to determine the local facet temperature. Strategies for measuring the facet temperature include the following: *Raman microprobe microscopy* [22] which relies upon measuring the Stokes/anti-Stokes phonon line intensity ratio. A drawback of this technique is it tends to be very slow and is typically limited to an accuracy of ±20 K. Also, the relatively high excitation laser power may itself cause heating of the facet, thereby obscuring the actual facet temperature. Since this is effectively a CW measurement it may itself impede COD from occurring at all. Since it will be unable to register the temperature during a pulse, the measured facet temperature may consequently be an average rather than a peak value. *Micro-Photomodulated reflectance* (μPR) is a variation on photoreflectance where only a very small sample area is investigated [23]. μ-PR can be used to monitor the facet temperature since the facet temperature can be related to the change in facet reflectivity. This is a very rapid measurement technique but experimentally very challenging as it requires very accurate alignment of an external laser on the laser facet. This introduces an error whereby the measured temperature may not exactly coincide with the temperature at the peak of the semiconductor laser optical mode. Furthermore, since this technique also uses an incident excitation laser, this may cause some facet heating itself and suffers from the same averaging effect as discussed above. The technique used for this paper relies on measuring the *high energy facet electroluminescence* emitted from the laser facet itself [24]. This technique utilizes the semiconductor emission itself as a means of determining the facet temperature. While this is a reasonably straightforward technique it can be time-consuming (up to one hour per measurement). In this experiment, the very high energy Boltzmann tail of the amplified spontaneous emission is measured. One of the major strengths of this technique is that it can be performed with the laser driven in either pulsed or CW mode. Under pulsed operation, internal self-heating of the laser is minimized (see later), allowing the laser to reach high optical power densities at the facet. With this technique, the facet temperature is, therefore, determined during the short pulse (while the instantaneous output power is high) so that the facet temperature can be measured close to the point of COD.

The basic idea of this technique can be understood as follows. From simple theory, it can be shown [24] that the rate of spontaneous emission r for a given photon energy, E may be written as

$$r = \alpha\Gamma\psi \exp\left(\frac{E_{fc} - E_{fv}}{kT}\right) E^2 \exp\left(\frac{-E}{kT}\right) \tag{1}$$

providing that E is several kT larger than the energy separation between the two quasi-Fermi levels, $E_{fc} - F_{fv}$. Here, k is Boltzmann's constant and ψ is a constant. Γ is the optical confinement factor in the cavity for light of energy E (the proportion of the flux overlapping the active region) and α is the effective bulk absorption coefficient at energy E. The coefficient α makes this expression very complicated since it varies with energy in an unknown manner depending on the joint density of states and the matrix elements which determine the optical transitions between the conduction and valence bands. However, if we consider *only* light being emitted from the end facet, this will have been guided along the laser cavity and have suffered re-absorption. Thus, if we assume that the laser is being uniformly pumped so that $E_{fc} - F_{fv}$ is a constant, we may write L, the number of photons of energy E emitted by the facet, as

$$L = \int_0^\infty \psi' \alpha\Gamma E^2 \exp\left(\frac{-E}{kT}\right) \exp(-\alpha\Gamma x) dx \tag{2}$$

where x is the distance along the laser cavity. The value of this integral is simply

$$L = \psi'' \alpha\Gamma \frac{1}{\alpha\Gamma} E^2 \exp\left(\frac{-E}{kT}\right) \tag{3}$$

and thus both α and Γ cancel to leave a simple expression for L where

$$L \propto E^2 \exp\left(\frac{-E}{kT}\right). \tag{4}$$

Thus, a plot of $\ln(\mathrm{L/E^2})$ against E is just a straight line of gradient −(1/kT) yielding the absolute temperature T. Γ typically varies from about 1%–3% per well for E just above the ground state to about 30% for light of energy E greater than the bandgap of the barrier material resulting in the observation of light from ∼10-20 μm to ∼ 1 μm, respectively. In practice, a large temperature gradient extends from the facet toward the bulk of the laser. This means that it is very difficult to obtain sensible temperature measurements based upon the QW emission (unless more sophisticated analysis is used [25]). However, due to the higher photon energy and correspondingly larger absorption coefficient, the light emitted from the barrier/SCH layers that is ultimately detected will only have come from a region

Authorized licensed use limited to: University of Surrey. Downloaded on May 26, 2009 at 10:09 from IEEE Xplore. Restrictions apply.

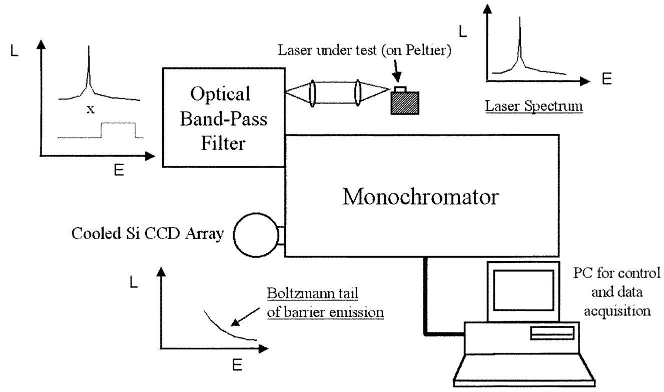

Fig. 2. Triple-spectrometer setup used to measure the high energy emission from the laser facet. Laser emission is first passed into the optical band-pass filter which selects only the high energy tail of the emission spectrum. This is then passed into a monochromator and dispersed onto a cooled silicon CCD array detector. The whole system is controlled via a PC.

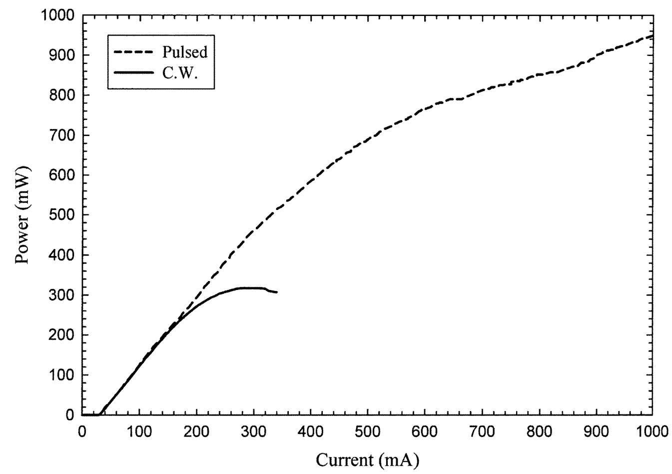

Fig. 3. Example of the power–current characteristic of a 980-nm laser under pulsed (dashed line) and CW (solid curve) operation. Under CW operation, due to joule heating caused by the injected current, the power rolls over with increasing current. However, under pulsed operation, the peak power can increase further due to the much reduced joule heating. One can observe COD more easily under pulsed operation due to the higher peak power.

very close to the facet. Hence, by measuring the tail of the barrier emission, the temperature in the vicinity of the facet may be determined.

IV. Measurement Technique

In a typical experiment on a 980-nm laser with GaAs barrier/waveguide layers, in order to extract the facet temperature it is necessary to examine the emission spectrum several kT above the GaAs emission peak. For the purposes of this investigation it was, therefore, deemed necessary to look at the emission present over the wavelength range $700 \leq \lambda \leq 800$ nm. Experimentally, this poses two problems. Firstly, the emission at these short wavelengths is considerably weaker than the peak intensity at 980 nm, $\sim 10^5 - 10^{10}$ times less intense, depending on the drive current. This itself gives rise to detection problems due to the low photon count. Associated with this, due to the much higher photon count at the 980-nm emission peak, scatter of light within a spectrometer can lead to severe distortions in the spectra at the shorter wavelengths. Thus, conventional optical spectrum analyzers proved to be unsuitable for this type of measurement. Instead, a Spex triple spectrometer together with a liquid nitrogen cooled CCD array was used as shown in Fig. 2. The triple spectrometer is configured as an optical band pass filter followed by a single monochromator. The optical band pass stage selects the spectral region of interest and rejects all other emission including the laser line at 980 nm. This filtered light is then fed into the monochromator and dispersed onto the high sensitivity liquid-nitrogen cooled silicon CCD array.

The lasers were bonded and mounted on T0–style headers incorporating a tungsten–copper heat sink. The base temperature was maintained at 25 °C using a Peltier effect thermoelectric heater/cooler system. The lasers were driven under both pulsed and CW operation using an ILX-LDP3811/3 and a ILX LDC3220, respectively. For the pulsed measurements, 500-ns long pulses were used at a repetition rate of 10 kHz. Fig. 3 shows an example of a power-current characteristic under pulsed (dashed line) and CW (solid line) operation. Note that the measured power under pulsed operation is the power over the duration of the pulse. Pulsed measurements minimize current (Joule) heating effects and hence one can achieve higher instantaneous optical power levels compared with CW operation. Joule heating can contribute to both overall device heating and may also reduce the facet temperature due to the reduced optical power for a given current. Thus, in practice it is easier to observe COD when driving a laser under pulsed mode. A drawback of using pulsed current is that it increases the duration of the experiment since longer scan times become necessary to achieve a sufficient time-averaged power level. Typically, the CW measurements took between 30 s and 1 h, depending on the drive current. When performing pulsed measurements there is a compromise between minimizing the level of noise and reducing the duration of the experiment. Thus, the pulsed measurements took approximately twice as long as the CW measurements to obtain reasonable, albeit significantly noisier spectra.

The devices studied were all 1-mm long with a 3-μm ridge tapering to either 6 or 9 μm. The active regions for both sets of devices consisted of two, ~1.5% compressively strained InGaAs QWs within GaAs barriers and a GaAs separate confinement heterostructure. The cladding layers were composed of $\mathrm{Al_{0.25}Ga_{0.75}As}$ with a graded interface. The structures were grown by metal–organic chemical vapor deposition (MOCVD) on n-doped GaAs substrates. Further details of the structures are given elsewhere [14]. It should be noted that the experimental devices selected for this investigation were fabricated with the aim of investigating aspects of design optimization including tapers and did not include the coatings or facet treatments used in production devices to combat COD.

V. Results and Discussion

A. CW Measurements

In Fig. 4, we show a typical spectrum for a 6-μm-wide tapered laser driven CW at a current of 20 mA (below laser threshold, $I_{\rm th}$). In the inset of Fig. 4 we show the part of the spectrum

Authorized licensed use limited to: University of Surrey. Downloaded on May 26, 2009 at 10:09 from IEEE Xplore. Restrictions apply.

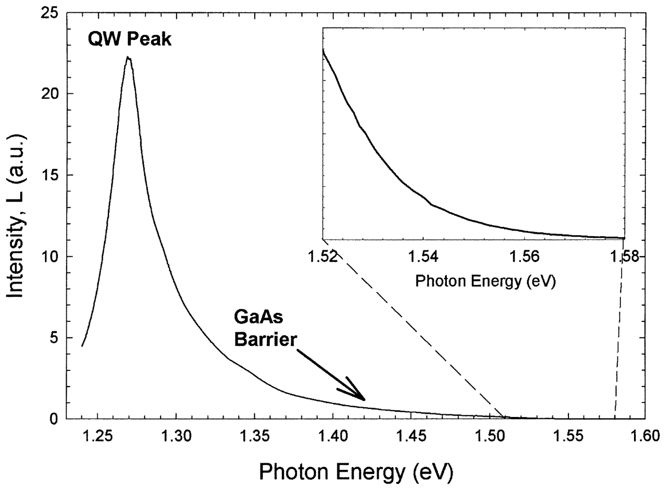

Fig. 4. Typical emission spectrum showing the QW emission peak and the high energy emission tail (inset) from the GaAs barrier layers from which the facet temperature may be extracted.

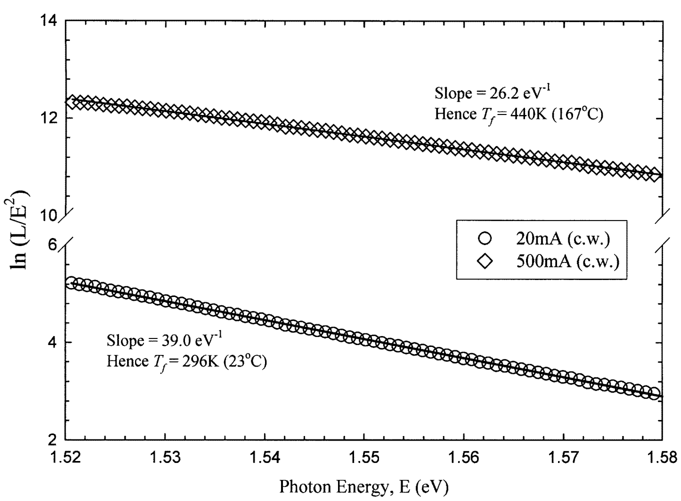

Fig. 5. Plot of $ln(L/E^2)$ versus E using the high energy Boltzmann tail of the facet emission at 20 (circles) and 500 mA (diamonds) for a 6-μm taper device under CW operation. From the slope of the plots, the facet temperature T_f can be deduced. Here, we find that at 20 mA (below $I_{\rm th}$) $T_f = 23$ °C which is in good agreement with the base temperature of 25 °C. At 500 mA, the decrease in slope corresponds to a facet temperature of 167 °C. This clearly shows a strong increase in facet temperature under high-power operation.

corresponding to the tail of the GaAs barrier emission which has been isolated using the bandpass of the triple spectrometer. In Fig. 5, this data is replotted in the form $ln(L/E^2)$ versus E where the measured data is given by the circles. It can be seen that over this energy range the plot is linear and upon performing a least squares linear fit (solid line) to the data we obtain a value for the gradient $(= 1/kT)$ and hence the temperature which we find to be 23 °C. This is in close agreement with the fixed substrate temperature of 25 °C and indicates an error in our measurement of about ± 2 °C. The diamonds represent the corresponding data for the laser driven at a CW current of 500 mA $(\sim 12I_{\rm th})$ corresponding to an output power $\sim$300 mW. Again, we observe a linear variation albeit with a shallower gradient. From this gradient we deduce a facet temperature of 167 °C. Clearly, therefore, under high power operation one can measure a significant increase in the local laser facet temperature. In Fig. 6, for many such measurements we plot the variation of the extracted facet temperature for devices with both a 6- (squares) and a 9-μm (circles) taper as a function of: (a) CW drive current and (b) measured output power. The dashed line indicates the temperature of the laser base maintained using the Peltier system. From Fig. 6(a), we observe that at low currents $(< 2I_{\rm th})$ the laser facet temperature initially remains approximately equal to the base temperature. However, with increasing current, the temperature increases superlinearly up to a maximum of 167 and 140 °C for the 6- and 9-μm taper devices at 500 mA, the highest current achievable with the current source. From this graph it would seem that the wider 9-μm taper device is indeed reducing the heating at the facet. However, in Fig. 6(b), where we plot the facet temperature as a function of output power, there appears to be little difference between the 6- and 9-μm taper devices. The reason for this can be seen in Fig. 7 where we plot the near-field $1/e^2$ width as a function of current for the 6- and 9-μm taper devices. At low currents we

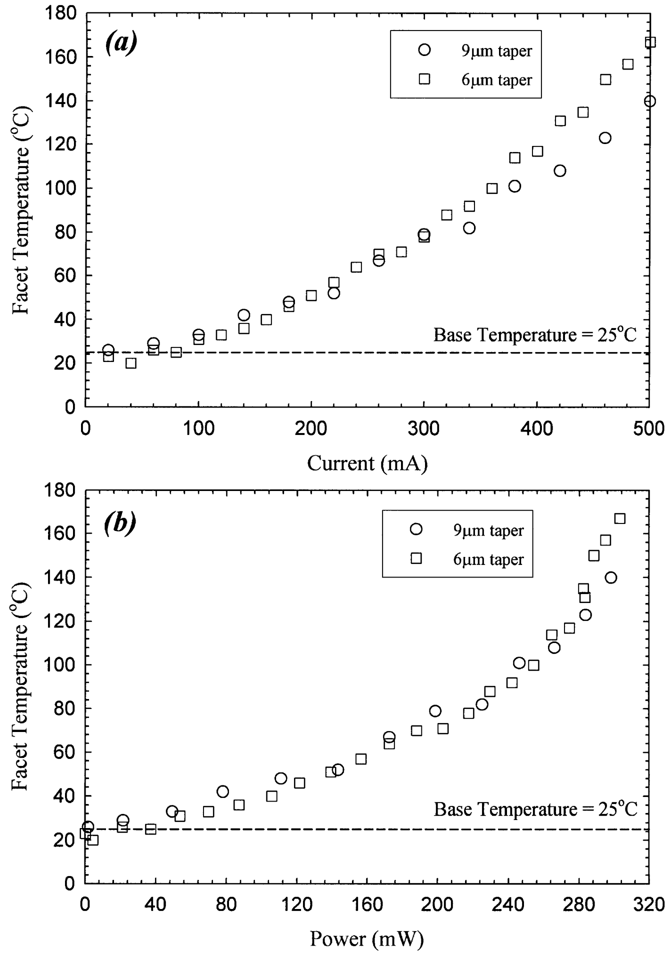

Fig. 6. (a) Variation in extracted facet temperature as a function of CW current for the 6- (squares) and 9-μm (circles) taper devices. At low currents, the facet temperature remains approximately equal to the base temperature; however, with increasing current, the temperature increases significantly up to 167 °C and 140 °C for the 6- and 9-μm taper devices, respectively. (b) Same data is plotted as a function of output power. Interestingly, in this plot there is little difference between the two sets of data. This suggests that there is, in fact, little difference in the facet power density for the two structures.

Authorized licensed use limited to: University of Surrey. Downloaded on May 26, 2009 at 10:09 from IEEE Xplore. Restrictions apply.

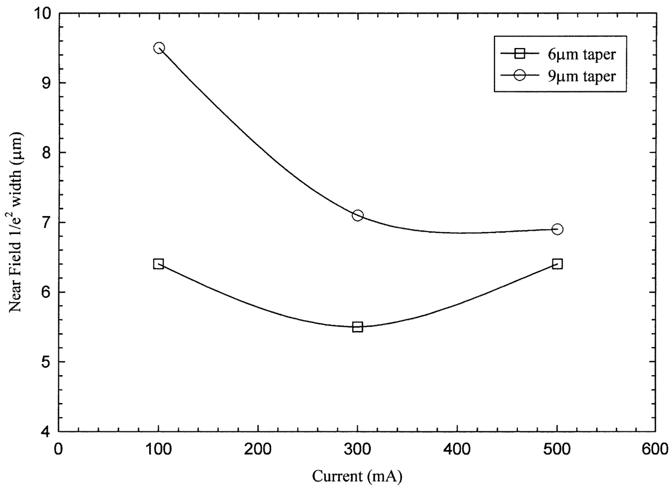

Fig. 7. Measured $1/e^2$ near field widths for the 6- (squares) and 9-μm (circles) taper devices as a function of CW current. While the mode width of the 6-μm taper device remains relatively constant with increasing current, the mode width decreases significantly for the 9-μm taper device with increasing current such that the two devices have similar mode widths at high current. This explains why there is little difference in the facet temperature as a function of power for the two devices.

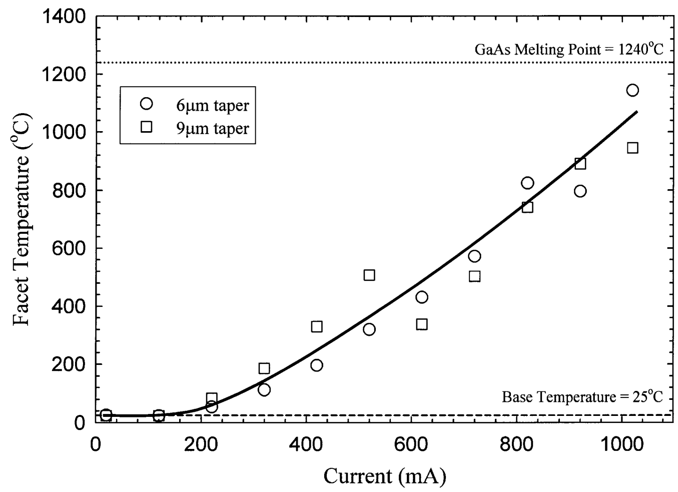

Fig. 8. Variation in facet temperature as a function of pulsed current for the 6- (circles) and 9-μm (squares) taper devices. Solid line is a guide to the eye. We observe that for both devices, above ~120 mA, the facet temperature increases sharply with current such that by 500 mA, $T_f \sim 400$ °C. This is higher than the corresponding CW current due to the higher output power under pulsed operation. Increasing the current further leads to further heating such that by 1000 mA, $T_f \sim 1000$°C. Beyond this current, both devices underwent COD. Dotted line indicates the melting point of GaAs. Rate of increase of facet temperature with current is consistent with the facet melting at COD.

observe that the $1/e^2$ width is approximately equal to the taper width. However, with increasing current the two widths appear to converge such that at 500 mA, the near field widths are almost equal in size. Therefore, with increasing current, there is little difference in the mode size and hence the optical power density for the two devices is approximately equal. Thus, in terms of facet heating, the devices behave similarly at high power. This result suggests that the 1-mm-long tapered cavity is insufficient to allow the mode to expand under high power operation and indicates the need to use devices with longer taper lengths.

B. Pulsed Measurements

From the CW measurements we clearly observed significant heating of the laser facet. However, as discussed earlier in this paper (and shown in Fig. 3), due to self-heating of the active region, the power–current characteristic under CW operation tends to roll over and, hence, one cannot observe catastrophic failure of the facet. Under pulsed operation one can achieve considerably higher power levels over the duration of the pulses. In Fig. 8, we plot the variation of the facet temperature with pulsed current for the 6- and 9-μm taper devices. The solid line is intended as a guide to the eye. While the data is clearly noisier, it does show that under pulsed operation, the facet temperature increases very sharply with current. At low current (up to 120 mA) the facet temperature (24 °C–26 °C) is approximately equal to the base temperature for both taper width devices. For a further increase in current the facet temperature increases superlinearly such that by 500 mA, the facet temperature is $\sim 400(\pm 100)$ °C. Even allowing for this large error, it is clear that under pulsed operation the heating is considerably higher than under CW operation [Fig. 6(a)] for which the facet reached a temperature of 140–167 °C. The apparent decrease in facet temperature between 500 and 600 mA for the 9-μm taper device may be caused by spatial hole burning whereby the laser then oscillates in a higher order mode resulting in a decrease in the facet power density. By further increasing the pulsed current the facet temperature continued to increase such that at 1000 mA $(\sim 25I_{\rm th})$, the facet temperature ~ 1000 °C. When the current was further increased to 1100 mA, both devices underwent COD. The dashed line in Fig. 8 shows the melting point of GaAs at atmospheric pressure (1240 °C). Our results confirm that the laser facet reached in excess of 1000 °C at COD, consistent with the melting point of the semiconductor itself. Interestingly, these results show that the facet temperature increases steadily with increasing current close to the point of COD.

VI. Conclusion

In summary, we have outlined and demonstrated a practical technique for measuring the facet temperature of a semiconductor laser under high-power operation. By applying this technique to 6- and 9-μm 1-mm-long tapered 980-nm lasers we measure a large increase in facet temperature under CW and pulsed operation. Under CW operation, the facet temperature increases from ~ 25 °C at low currents to over 140 °C at 500 mA. We found little difference in facet temperature between the devices with respect to output power. This is due to the fact that the near field width of the devices is approximately equal at high power. Hence, for 1-mm-long devices, there is, in fact, little difference in optical power density at the facet. From pulsed measurements we observe a sharper rise in facet temperature as a function of current (~ 400°C at 500 mA) when compared with the CW measurements. This arises due to self-heating under CW operation which limits the output power and hence facet heating due to the overall device Joule heating. Under pulsed operation the maximum measured facet temperature was in excess of 1000 °C for a current of 1000 mA. Beyond this, both lasers underwent

Authorized licensed use limited to: University of Surrey. Downloaded on May 26, 2009 at 10:09 from IEEE Xplore. Restrictions apply.

COD. This was made possible by measuring the facet heating during the pulse itself. These results demonstrate that the laser facet temperature increases sharply with current/power and is consistent with the facet melting at COD at a temperature comparable with the melting point of GaAs.

ACKNOWLEDGMENT

The authors would like to thank Dr. R. Beanland for producing the SEM images shown in this paper and Dr. D. Lancefield for assistance with the triple spectrometer. They also would like to thank the laser team at Bookham Technology PLC, Caswell, for the fabrication and supply of the lasers used in this study.

REFERENCES

[1] D. F. Welch, "A brief history of high-power semiconductor lasers," *IEEE J. Select. Topics Quantum Electron.*, vol. 6, pp. 1470–1477, 2000.
[2] H. Horie, H. Ohta, and T. Fujimori, "Reliability improvement of 980-nm laser diodes with a new facet passivation process," *IEEE J. Select. Topics Quantum Electron.*, vol. 5, pp. 832–838, 1999.
[3] J.-I. Hashimoto, N. Ikoma, M. Murata, J. Fukui, T. Nomaguchi, and T. Katsuyama, "Surface treatment by Ar plasma irradiation in electron cyclotron resonance chemical vapor deposition," *Jpn. J. Appl. Phys.*, vol. 39, pp. 2761–2766, 2000.
[4] A. Valster, A. T. Meney, J. R. Downes, D. A. Faux, A. R. Adams, A. A. Brouwer, and A. J. Corbijn, "Strain-overcompensated GaInP-AlGaInP quantum-well laser structures for improved reliability at high-output powers," *IEEE J. Select. Topics Quantum Electron.*, vol. 3, pp. 180–187, 1997.
[5] T. Fukunaga, M. Wada, and T. Hayakawa, "High-power 0.8 μm InGaAsP/InGaP/AlGaAs single quantum well lasers with tensile-strained InGaP barriers," *Jpn. J. Appl. Phys.*, vol. 38, pp. L387–L389, 1999.
[6] A. R. Adams, A. T. Meney, J. R. Downes, A. Valster, and G. A. Acket, "Semiconductor diode laser and method of manufacturing same," U.S. Patent 5 956 359, 1999.
[7] M. Sagawa, K. Hiramoto, T. Toyonaka, T. Kikawa, S. Fujisaki, and K. Uomi, "Highly reliable and stable-lateral-mode operation of high-power 0.98-μm InGaAs-InGaAsP lasers with an exponential-shaped flared stripe," *IEEE J. Select. Topics Quantum Electron.*, vol. 3, pp. 666–671, 1997.
[8] G. W. Yang, R. J. Hwu, Z. T. Xu, and X. Y. Ma, "High-performance 980-nm quantum-well lasers using a hybrid material system of an Al-free InGaAs-InGaAsP active region and AlGaAs cladding layers grown by metal-organic chemical vapor deposition," *IEEE J. Quantum Electron.*, vol. 35, pp. 1535–1541, 1999.
[9] M. Sagawa, T. Toyonaka, K. Hiramoto, K. Shinoda, and K. Uomi, "High-power highly-reliable operation of 0.98-μm InGaAs-InGaP strain-compensated single-quantum-well lasers with tensile strained InGaAsP barriers," *IEEE J. Select. Topics Quantum Electron.*, vol. 1, pp. 189–195, 1995.
[10] J. K. Lee, K. H. Park, D. H. Jang, H. S. Cho, C. S. Park, K. E. Pyun, and J. Jeong, "Improvement of Catastrophic Optical Damage (COD) level for high-power 0.98-μm GaInAs-GaInP laser diodes using impurity induced layer disordering," *IEEE Photon. Technol. Lett.*, vol. 10, pp. 1226–1228, 1998.
[11] J.-I. Hashimoto, N. Ikoma, M. Maruta, and T. Katsuyama, "A highly reliable GaInAs-GaInP 0.98-μm window laser," *IEEE J. Quantum Electron.*, vol. 36, pp. 971–977, 2000.
[12] F. R. Gfeller, P. Buchmann, P. W. Epperlein, H. P. Meier, and J. P. Reithmaier, "High-power single-mode AlGaAs lasers with bent-waveguide nonabsorbing etched-mirrors," *J. Appl. Phys.*, vol. 72, pp. 2131–2135, 1992.
[13] D. Botez, "Semiconductor laser with non-absorbing mirror facet," U.S. Patent 4 523 316, 1985.
[14] *Proc. 1998 Institute Physics Semiconductor Integrated Optoelectronics Conf.*, Cardiff, U.K..
[15] J. C. Brice, *Properties of GaAs*, 2nd ed. London, U.K.: INSPEC, 1991, p. 20.
[16] C. H. Henry, P. M. Petroff, R. A. Logan, and F. R. Merritt, "Catastrophic damage of $Al_xGa_{1-x}As$ double-heterostructure material," *J. Appl. Phys.*, vol. 50, pp. 3721–3732, 1979.
[17] S. Adachi, *Physical Properties of III–V Semiconductor Compounds, InP, InAs, GaAs, GaP, InGaAs, and InGaAsP*. New York: Wiley, 1992, p. 58.
[18] G. P. Agarawal and N. K. Dutta, *Long Wavelength Semiconductor Lasers*. New York: Van Nostrand Reinhold, 1986, pp. 115–116.
[19] S. J. Sweeney, A. F. Phillips, A. R. Adams, E. P. O'Reilly, and P. J. A. Thijs, "The effect of temperature dependent processes on the performance of 1.5 μm compressively strained InGaAs(P) MQW semiconductor diode lasers," *IEEE Photon. Technol. Lett.*, vol. 10, pp. 1076–1078, 1998.
[20] A. F. Phillips, S. J. Sweeney, A. R. Adams, and P. J. A. Thijs, "The temperature dependence of 1.3-μm and 1.5-μm compressively strained InGaAs(P) MQW semiconductor lasers," *IEEE J. Select. Topics Quantum Electron.*, vol. 5, pp. 401–412, 1999.
[21] P. G. Eliseev, "Optical strength of semiconductor laser materials," *Prog. Quantum Electron.*, vol. 20, pp. 1–82, 1996.
[22] S. Todoroki, "Influence of local heating on current-optical output power characteristics $InGa_{1-X}Al_xAs$ lasers," *J. Appl. Phys.*, vol. 60, pp. 61–65, 1986.
[23] P.-W. Epperlein, "Micro-temperature measurements on semiconductor laser mirrors by reflectance modulation: A newly developed technique for laser characterization," *Jpn. J. Appl. Phys.*, vol. 32, pp. 5514–5522, 1993.
[24] A. R. Adams, E. Cariou, P. Vicente, B. Couzinet, and A. Raymond, "Measurement of the well and facet temperatures of normally operating quantum well lasers by analysis of the spontaneous emission from the facets," in *Proc. 7th Eur. Conf. Integrated Optics (ECIO'95)*, 1995, pp. 121–124.
[25] P. E. L. Fermor and A. R. Adams, "A theoretical analysis of the influence of well and facet temperatures on the facet emission spectra of normally operating quantum well lasers," in *Proc. Institute Physics, 1998 Condensed Matter Materials Physics Conf.*, Manchester, U.K..

Stephen John Sweeney (S'98–M'99) was born in Luton, U.K., in 1973. He received the B.Sc. (Hons.) degree in applied physics and the Certificate in Education from the University of Bath, Bath, U.K., in 1995 and the Ph.D. degree in semiconductor laser physics at the University of Surrey, Surrey, U.K., in 1999.

After two years as a Postdoctoral Researcher he worked as a Scientist for Marconi Optical Components on the development of signal and pump sources for telecommunications applications. He is currently a Lecturer in semiconductor laser physics at the University of Surrey. His research interests include understanding the gain and loss processes underpinning the performance of semiconductor lasers utilizing a combination of novel experimental techniques coupled with complementary theoretical modeling. His current research activities include long-wavelength InGaAs(P)-, AlGaInAs-, and GaInNAs-based MQW semiconductor lasers for cooler-free applications and future GaAs-based vertically integrated devices. He is also interested in failure mechanisms in high power semiconductor lasers for fiber amplifiers and has worked on both visible VCSEL and edge-emitting lasers as well as 1.3-µm quantum dot structures.

Dr. Sweeney is a Chartered Physicist and a member of The Institute of Physics, London, U.K.

Leslie Jamieson Lyons was born in Edinburgh, U.K., in 1978. He received the M.Phys. (Hons.) degree in physics from Heriot-Watt University, U.K., in 1999, studying also at l'Ecole Nationale Supérieure de Physique de Marseille, France, as part of this degree.

In June 2000, he joined Marconi Caswell Technology (now Bookham Technology) where he is engaged in the research of telecommunications semiconductor laser devices.

Authorized licensed use limited to: University of Surrey. Downloaded on May 26, 2009 at 10:09 from IEEE Xplore. Restrictions apply.

Alfred R. Adams (M'82–SM'00–F'01) was born in the U.K., in 1939. He received the B.Sc., Ph.D., and D.Sc. degrees in physics from the University of Leicester, Leicester, U.K., in 1961, 1964, and 1986, respectively. After completing his Ph.D. research into the electrical and optical properties of orthorhombic sulphur he spent two years at the University of Karlsruhe, Karlsruhe, Germany, studying the thermal and thermoelectric properties of selenium and tellurium.

In 1967, he joined the University of Surrey, Surry, U.K., where he is now a Professor of physics and Leader of the Optoelectronic Devices and Materials research group. Semiconductor lasers have been one of his major interests since 1980 when he spent sabbatical leave at Tokyo Institute of Technology, Tokyo, Japan. He held the Hitachi Visiting Chair at Tokyo Institute of Technology in 1992 and was CNRS Visiting Researcher at the University of Montpellier in 1993.

Dr. Adams was awarded the Duddell Medal and Prize by the Institute of Physics, U.K., in 1995 for his work on strained-layer lasers. He is a Fellow of the Institute of Physics, London, U.K., and the Institute of Electrical Engineers, U.K. In 1996, he was Elected Fellow of the Royal Society.

Daren Alfred Lock was born in Towcester, U.K., in 1968. He received the B.Sc. (Hons.) degree in physics with nuclear astrophysics from the University of Surrey, Surrey, U.K., in 2000. He is currently working toward the Ph.D. degree at the University of Surrey.

His research interests include experimental methods to investigate the underlying processes involved in catastrophic optical damage and high power recombination effects in semiconductor lasers for fiber amplifiers.

Mr. Lock is an Associate Member of the Institute of Physics, London, U.K.

Authorized licensed use limited to: University of Surrey. Downloaded on May 26, 2009 at 10:09 from IEEE Xplore. Restrictions apply.